Available online at www.sciencedirect.com
SCIENCE DIRECT
Sensors and Actuators A 130–131 (2006) 48–53
SENSORS AND ACTUATORS A PHYSICAL
www.elsevier.com/locate/sna

Integrating wireless ECG monitoring in textiles

Johan Coosemans *, Bart Hermans, Robert Puers

Katholieke Universiteit Leuven, Department ESAT-MICAS, Kasteelpark Arenberg 10, B-3001 Leuven-Heverlee, Belgium

Received 20 June 2005; received in revised form 13 October 2005; accepted 20 October 2005
Available online 20 December 2005

Abstract

This paper reports on the full realization of a garment embedded patient monitoring system, including wireless communication and inductive powering. The developed system is primarily intended for the continuous monitoring of the electrocardiogram (ECG) of children with an increased risk of Sudden Infant Death Syndrome (SIDS). The sensors and the antenna are made out of textile materials. All electronics are mounted on a flexible circuit to facilitate integration in the baby's pajamas. A significant increase in the comfort of patient and nursing staff is achieved by this integration in textiles. A prototype baby suit was fabricated and successfully tested.

Keywords: ECG; Intelligent textiles; Inductive powering; Telemetry

1. Introduction

Previous work on so-called 'intelligent textiles' shows that biomedical monitoring systems can greatly benefit from the integration of electronics in textile materials [1–8]. This synergy between textiles and electronics mainly originates from the fact that clothing is our most natural interface to the outside world. The higher the level of integration of the sensors and circuits in the clothing, the more unnoticeable the monitoring system becomes to its user and thus the higher the comfort of the user.

This paper presents a garment embedded patient monitoring system, primarily intended for the monitoring of babies prone to Sudden Infant Death Syndrome (SIDS). As these babies have an increased risk of cardiac arrest, a continuous measurement of the electrocardiogram (ECG) is necessary. Up to now adhesive gel electrodes are used, wired to an alarm unit. These wires hinder both the baby and the nursing staff. Furthermore, the long-term use of conventional gel electrodes can cause skin irritation and allergic contact reactions. This paper presents a solution that overcomes these inconveniences by the integration of the sensors, interconnects and the processing and transmission circuitry in the baby's suit. A general system overview is depicted in Fig. 1.

2. ECG measurement

As an alternative to conventional ECG electrodes, both knitted and woven stainless steel electrodes (called Textrodes) were developed in collaboration with Bekintex [8]. These dry Textrodes (Fig. 2) are less irritating than gel electrodes. In addition, stainless steel has a low toxicity, the yarns can be manipulated as a textile material, and can be washed without losing their properties. Disadvantages of the Textrodes however, are the increased sensitivity to motion artifacts, as well as the poor skin–electrode contact. Therefore, the analog ECG front-end had to be redesigned.

Because the Textrodes are of bad quality, a three-electrode ECG configuration circuit is preferred over a two-electrode ECG circuit. In a first attempt, a driven right leg (DRL) topology (see Fig. 3) was implemented, because of its known high common mode rejection ratio (CMRR) [9]. Fig. 4 (left) shows the equivalent circuit, for the calculation of the common mode interference.

In this equivalence, it is supposed that all electrode impedances Z_e are equal and that the amplifier's poles do not lie in the aimed frequency range (0.5–150 Hz). The common

* Corresponding author. Tel.: +32 16321716; fax: +32 16321975.
E-mail addresses: johan.coosemans@esat.kuleuven.be (J. Coosemans), robert.puers@esat.kuleuven.ac.be (R. Puers).

0924-4247/$ – see front matter © 2005 Elsevier B.V. All rights reserved.
doi:10.1016/j.sna.2005.10.052

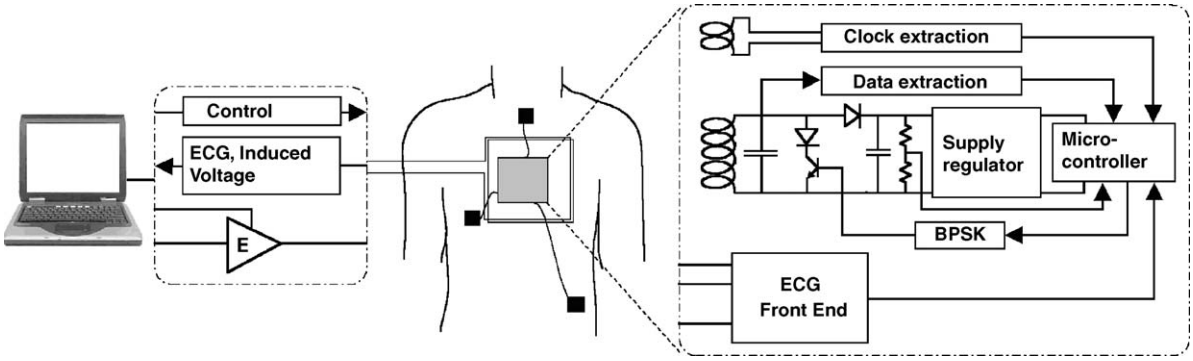

Fig. 1. General overview of the system.

mode voltage V_c is then given by:

$$V_c = \frac{s \cdot Z_g \cdot K \cdot (Z_e + Z_i)}{Z_i(1+A) + Z_e + Z_g + s \cdot Z_g + Z_g \cdot C_x \cdot (Z_e + Z_i)} \cdot V_p \quad (1)$$

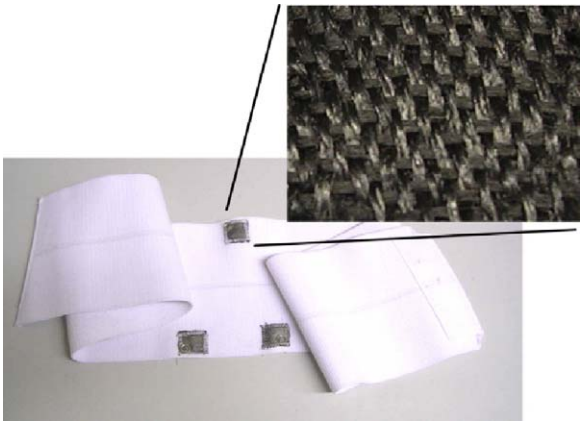

Fig. 2. Belt with Textrodes.

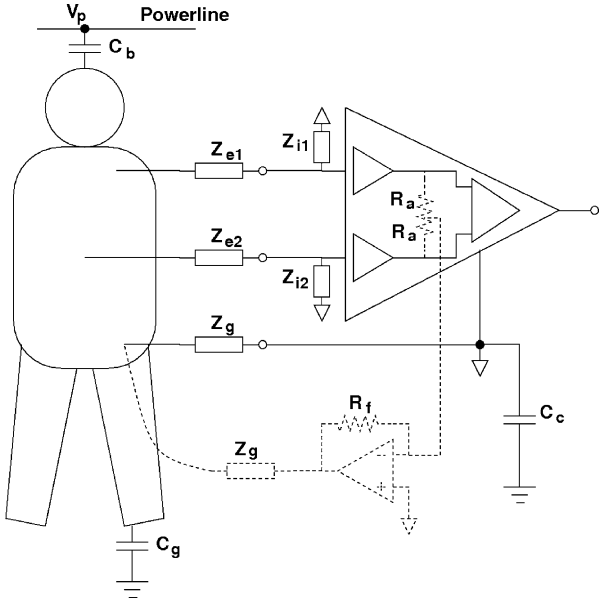

Fig. 3. Simplified model for thee-electrode ECG configuration. Dotted line: DRL; full line: grounded configuration.

with $Z_{e1} = Z_{e2} = 2Z_e$, the input impedances and $Z_{i1} = Z_{i2} = 2Z_i$, the DRL feedback gain A:

$$A = \frac{2 \cdot R_f}{R_a}, \quad C_x = \frac{C_c \cdot (C_g + C_b)}{C_g + C_b + C_c} \quad \text{and}$$

$$K = \frac{C_c \cdot C_b}{C_g + C_b + C_c}.$$

V_p is the common mode source, e.g. due to 50 Hz power-line interference.

Eq. (1) can be further simplified: the electrode impedances are much smaller than the input impedance of the amplifier (Z_e, $Z_g \ll Z_i$) and the pole in (1) lies out the frequency range of interest. Eq. (1) then becomes:

$$V_c = \frac{s \cdot Z_g \cdot K}{1 + A} \cdot V_p \quad (2)$$

We can make the same calculations for a grounded three-electrode configuration. In this case, the equivalent circuit for the calculation of the common mode is shown in Fig. 4 (right). The calculations then lead to:

$$V_c = \frac{s \cdot Z_g \cdot K \cdot (Z_e + Z_i)}{Z_i + Z_e + Z_g + s \cdot Z_g \cdot C_x \cdot (Z_e + Z_i)} \cdot V_p \quad (3)$$

Simplification yields:

$$V_c = s \cdot Z_g \cdot K \cdot V_p \quad (4)$$

From Eqs. (2) and (4), the advantage of the DRL configuration compared to the grounded configuration becomes clear. The common mode is reduced with a factor A, which is the gain of the feedback amplifier in the DRL configuration. To minimize the common mode interference, the gain A can be increased.

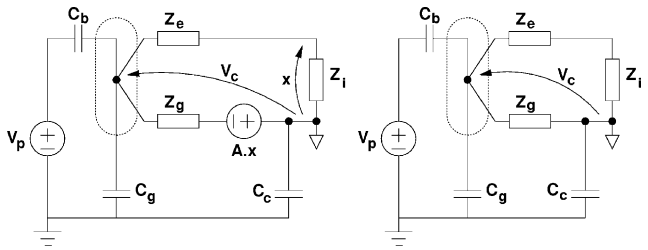

Fig. 4. Equivalent circuit for the common mode. Left: DRL; right: grounded configuration.

Nonetheless, saturation of the output of the feedback amplifier must be avoided.

In the presented design, the common mode signal does not only consist of 50 Hz power-line interference, but mainly originates from the electro-magnetic field that is used for the inductive powering of the circuit (as described in next paragraph). Measurements at the input of the ECG amplifier learned that the resulting common mode signal almost forces the opamp into saturation, due to the large RF field. Eq. (2) illustrates that the common mode of a DRL circuit can only be reduced if the feedback amplifier has a large gain. However, under the above mentioned common mode conditions, this gain must be limited to $A \approx 1$. Consequently the DRL circuit has only little outcome on the common mode rejection and becomes ineffective. For this reason, a grounded three-electrode configuration is implemented instead.

The design of this grounded configuration ECG amplifier is hampered by the presence of the RF field as well. For normal levels of common mode interference, a large amplification factor is implemented in the differential to single ended amplifier, to obtain a high signal-to-noise ratio. In this application however, the amplification in the first stages must be limited to avoid saturation due to the large common mode signal. The ECG amplifier is followed by a third-order low pass filter, with a cut-off frequency of 150 Hz, to eliminate the remaining RF common mode. The filter contains further distributed amplification.

3. Power and data transmission

Power is provided trough an inductive link at 132 kHz, so batteries can be left out. Continuous measurements, reduction of the volume and weight, and ease of package sealing are the key benefits of this approach. Fig. 5 shows a schematic overview of the inductive link and the equivalent non-coupled circuit. The power consumption of the system is represented by a load resistance R_{load}.

Starting form this equivalence, the link gain V_{sec}/V_1 can be calculated. This link gain reaches a maximum at the resonance frequency ω_r, with

$$\omega_r = \frac{1}{\sqrt{L_{s2} \cdot C}} = 132\,\text{kHz} \tag{5}$$

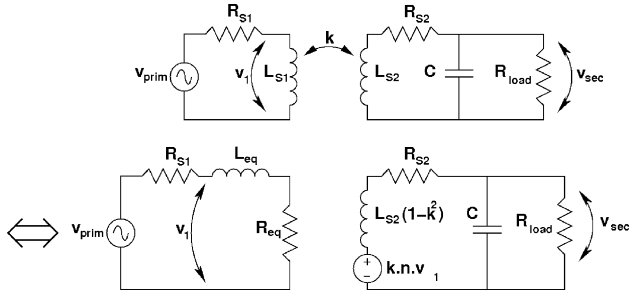

Fig. 5. Top: schematic overview of the inductive link. Bottom: equivalent non-coupled circuit.

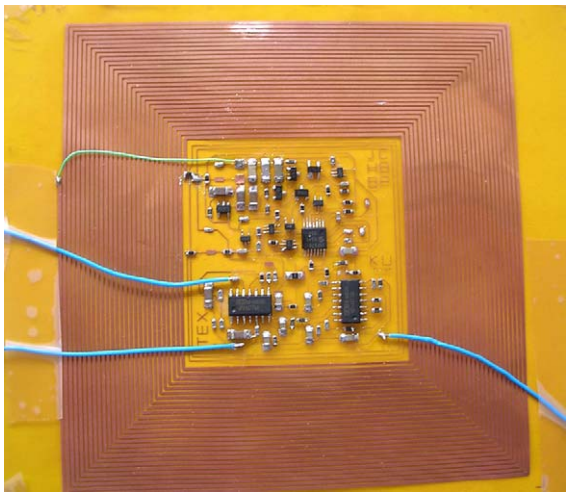

Fig. 6. Flexprint with integrated circuitry and secondary coil; 10 cm × 10 cm (70 μm Cu; $N = 27$).

The maximum gain equals:

$$\left|\frac{V_{sec}}{V_1}\right|_{max} \approx k \cdot n \cdot \left[\frac{1}{\frac{L_{s2}\cdot\omega_n}{R_{load}} + \frac{R_{s2}}{L_{s2}\cdot\omega_n}}\right] \quad (\text{for } R_{load} \gg R_{s2}) \tag{6}$$

where k is the coupling factor, n the transformer ratio and ω_n is the natural frequency, with

$$n = \sqrt{\frac{L_{s2}}{L_{s1}}} \quad \text{and} \quad \omega_n = \frac{1}{\sqrt{L_{s2} \cdot C}} \cdot \sqrt{1 + \frac{R_{s2}}{R_{load}}}.$$

The external coil is made large (26.5 cm × 26.5 cm × 2 cm), to cope with misalignments between the primary and secondary coil, e.g. due to movement of the baby. In a first prototype, the receiving coil is implemented together with all electronics on a flexible circuit (Fig. 6). The available area for this coil is about 10 cm × 10 cm. The number of turns N of this secondary coil was optimized in software to maximally exploit the available area and achieve a maximum link gain. This allows minimizing the radiated magnetic field strength.

From Eq. (6), the optimal number of turns N can be determined. A large N results in a large L_{s2} and consequently a large transformer ratio n. On the other hand, a large N also means that the coil windings become thin, resulting in a large R_{s2} and a low quality factor Q. The inductive link was simulated in FASTHENRY [10], for a mutual coil distance of 9 cm and $R_{load} = 500\,\Omega$. Fig. 7 shows the simulated link gain as a function of the number of turns, with a maximum at $N = 27$. Table 1

Table 1
Measurements and simulated values of the inductive link properties

	Simulated	Measured
L_{s1} (μH)	21.2	21.1
L_{s2} (μH)	82.4	82.7
Q_{s2} (at 132 kHz)	24.9	21.2
k (%)	4.63	4.7
V_{sec}/V_1	0.52[a]	0.47

Flexible printed circuit coil.
[a] Eq. (6).

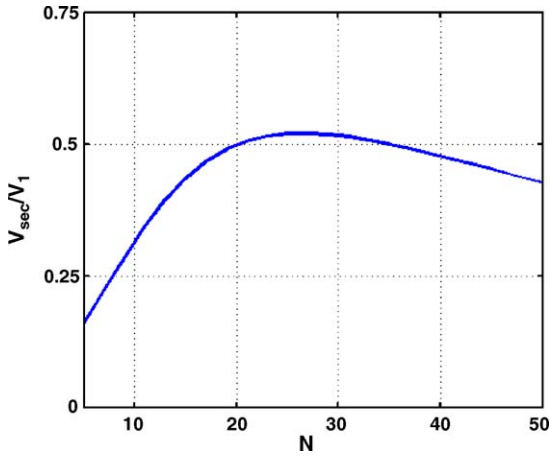

Fig. 7. Link gain as a function of the number of turns of the secondary coil.

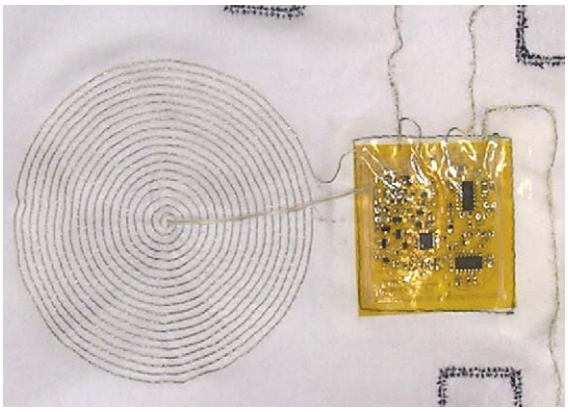

Fig. 9. Detail of the backside of the baby suit, showing the embroidered coil and the flexprint.

illustrates the good agreement between the simulations and measurements of the inductive link properties.

Wireless bi-directional data communication is provided through the same inductive link as the power transfer. The data transmission to the implant is used to adapt the measuring algorithm to the patient's specific needs and is done by on/off keying of the driver. The uplink to the receiver transmits the measured data and by load modulation. This passive telemetry is implemented based on the proven techniques in [11]. The ECG is sampled at 300 Hz. The transmission data rate is at 16.5 kbit/s.

After the inductive link optimization, the telemetric range extends up to an axial distance of 18 cm from the external coil that can be placed under the mattress. As the maximal range is not always demanded, an automatic power control is implemented to reduce unnecessary power dissipation. For this purpose, the induced voltage is measured at the input of the voltage regulator that regulates the supply voltage to 5 V (see Fig. 1). This voltage is sampled at 10 Hz and sent to the external unit. In case the induced voltage drops below 6 V or rises above 8 V, e.g. due to movement of the baby, the external unit will correct the transmitted power level. To this end the supply voltage of the class-E driver can be digitally controlled from 2 to 24 V.

4. Prototype fabrication

All electronics for the sensor interface, data processing and wireless transmission are mounted on a flexible printed circuit (Fig. 6). The substrate material (Dupont LF9210) consists of a laminate structure of Kapton polyimide (25 μm) and copper foil (70 μm) and is patterned by a standard photolithographic process. As the flexible printed circuit is highly compliant, it can be knitted in clothing without a reduction in comfort.

For the ease of fabrication, in a first prototype, the coil for inductive powering and data transmission is integrated on the flexible printed circuit as well (see Fig. 6). The thick copper layer results in a high quality coil (Table 1). The Textrodes are knitted in an elastic belt, which can be worn under the normal clothing. The elasticity of the belt assures a good contact between the body and the electrodes. The flexible circuit is connected to the electrodes by means of three press-studs. In this way, the electronics can easily be removed when the belt is to be washed.

In a second prototype, the secondary coil is embroidered on a baby suit (see Figs. 8 and 9). This further enhances the comfort of the baby, as the size of the non-breathing Kapton film can be reduced from 10 cm × 10 cm to 5 cm × 5 cm. The coil wire consists of 19 μm × (Ø 79 μm) stainless steel yarns with a copper

Fig. 8. Baby suit prototype. Left: inside showing the Textrodes; right: backside.

Fig. 10. Left: demo set-up with belt prototype, worn by a 12 weeks old baby. Right: baby suit prototype, worn by a 21 weeks old baby.

Table 2
Measurements and simulated values of the inductive link properties

	Simulated	Measured
L_{s2} (μH)	12.7	13.7
Q_{s2} (at 132 kHz)	18.3	17.2
k (%)	3.33	3.2
V_{sec}/V_1	0.34[a]	0.26

Embroidered coil.
[a] Eq. (6).

core and has a low resistance of 0.20 Ω/m. The extremities of the coil wire are directly soldered to the flexible circuit.

The connections from the circuit to the electrodes are embroidered in a similar way. Contact between the electrodes and interconnect wires is achieved by knitting the wire through the electrodes.

For this type of coil, the optimal number of turns ($N = 33$) is not feasible, as the winding density is limited by the embroidering technique. Table 2 compares measurements with simulated values of the inductive link properties for the baby suit prototype.

5. Results

The prototypes described above were successfully tested. A demo set-up with the belt prototype, worn by a 12 weeks old baby is depicted in Fig. 10 (left). A raw ECG measured in this set-up is shown in Fig. 11. No signal processing was applied. Fig. 10 (right) shows the baby suit prototype, worn by a 21 weeks old baby. The measurement results of both prototypes are similar. Fig. 12 depicts an ECG measured with the same set-up as in Fig. 11, except for using conventional electrodes instead of the Textrodes. The ECG signals measured with the Textrodes display more low frequent base line drift, and the signal-to-noise ratio is lower than when using conventional gel electrodes. Nonetheless, even with the Textrodes, the signal quality is more than adequate for an accurate beat-to-beat detection of the heart rate, as demanded by the application.

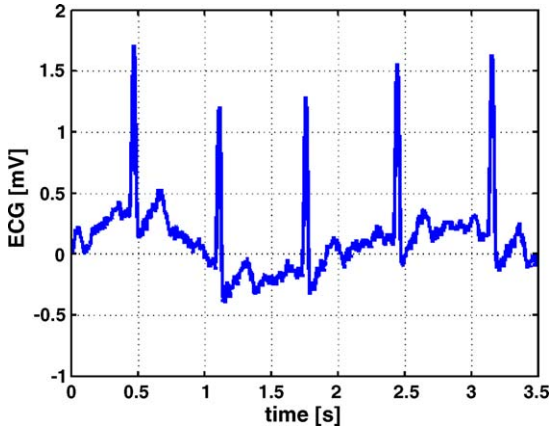

Fig. 11. ECG measured in set-up of Fig. 10 (left). Raw non-filtered data.

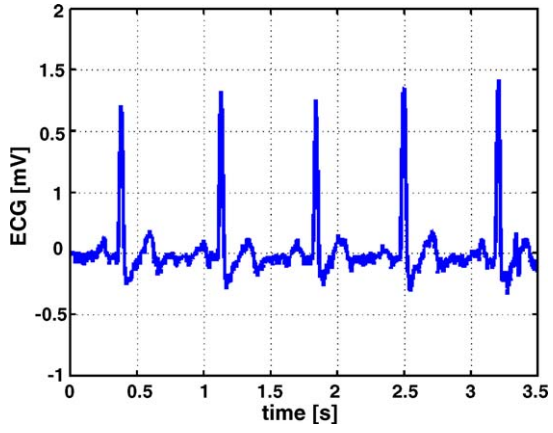

Fig. 12. ECG measured with the same set-up as in Fig. 11, except for using conventional electrodes instead of Textrodes.

6. Comparison with other monitoring suits

The field of ‘smart clothing’ is evolving rapidly: ambulatory monitoring suits are being developed by the University of Pisa [2], the University of Karlsruhe [3], Vivometrics [4] and the MyHeart consortium [5]. More specifically, SIDS suits for newborn are under development by Sensatex [6] and Verhaert [7].

The novelty of the system, presented in this paper, lies in the level of integration into textiles. Whereas few of the other systems also use textile sensors, none of them has an integrated solution for wireless communication and powering. In general, the instrumentation electronics, together with a battery and a wireless transceiver, are packaged in a 'box' that can be plugged to the shirt and that is to be removed before washing. By implementing inductive powering over a textile coil, we could downsize this 'box' to a single flexible circuit that can be rigidly connected to the fabric. In the future, the size of this flex can be further minimized by integration of the electronic components. So although a large effort remains to make the complete suit machine washable, a solution comes into sight, e.g. by molding [12] the miniaturized electronic module to the fabric.

7. Conclusion

The presented system has proven the feasibility of integrating sensors and electronics in textiles for measuring ECG, combined with wireless powering and data communication. Through these developments the comfort of the patient has entered a new dimension. Moreover, this is one of the first working demonstrators of wireless 'intelligent textiles'. Future work will focus on miniaturization of the electronics, packaging and further clinical validation.

Acknowledgements

Part of this research was conducted within the framework of the 'Intellitex' project, in collaboration with the Department of Textiles and the Department of Pediatrics and Genetics, Ghent University, and sponsored by the Institute for the Promotion of Innovation through Science and Technology in Flanders (IWT). Bekintex NV and ZSK GmbH are acknowledged for their support. J. Coosemans is a research assistant of the Fund for Scientific Research—Flanders (Belgium).

References

[1] D. Marculescu, R. Marculescu, N.H. Zamora, P. Stanley-Marbell, P.K. Khosla, S. Park, S. Jayaraman, S. Jung, C. Lauterbach, W. Weber, T. Kirstein, D. Cottet, J. Grzyb, G. Tröster, M. Jones, T. Martin, Z. Nakad, Electronic textiles: a platform for pervasive computing, in: Proceedings of the IEEE, vol. 91, 2003, pp. 1995–2018.
[2] D. De Rossi, F. Carpi, F. Lorussi, A. Mazzoldi, R. Paradiso, E.P. Scilingo, A. Tognetti, Electroactive fabrics and wearable biomonitoring devices, AUTEX Res. J. 3 (2003) 180–185.
[3] J. Ottenbacher, S. Römer, C. Kunze, U. Großmann, W. Stork, Integration of a bluetooth based ECG system into clothing, in: Proceedings of the Eighth IEEE International Symposium on Wearable Computers (ISWC'04), Arlington, VA, October 31–November 3, 2004, pp. 186–187.
[4] M. Coyle, Ambulatory cardiopulmonary data capture, in: Proceedings of the Second Annual International IEEE-EMBS Special Topic Conference on Microtechnologies in Medicine and Biology, Madison, WI, USA, May 2–4, 2002, pp. 297–300.
[5] MyHeart, 2005, http://www.hitech-projects.com/euprojects/myheart/.
[6] Sensatex, 2005, http://www.sensatex.com.
[7] Verhaert, 2005, http://www.verhaert.com.
[8] M. Catrysse, R. Puers, C. Hertleer, L. Van Langenhove, H. Van Egmond, D. Matthys, Towards the integration of textile sensors in a wireless monitoring suit, Sens. Actuators A 114 (2004) 302–311.
[9] J. Webster, Medical Instrumentation and Design, Houghton Mifflin Company, Boston, 1978, pp. 273–303.
[10] M. Kamon, M.J. Tsuk, J. White, FASTHENRY: a multipole-accelerated 3-D inductance extraction program, IEEE Trans. Microwave Theory Technol. 42 (1994) 1750–1758.
[11] J. Coosemans, R. Puers, An autonomous bladder pressure monitoring system, in: Digest of Technical Papers of the 18th European Conference on Solid-State Transducers (Eurosensors XVIII), Rome, Italy, September 12–15, 2004, pp. 211–212.
[12] T. Linz, C. Kallmayer, Integration of microelectronics into textiles, in: Proceedings of the Avantex Symposium 2005, on CD, Frankfurt, Germany, June 7–9, 2005.

Biographies

Johan Coosemans was born in Wilrijk, Belgium, in 1978. He received his MS degree in microelectronics from the Katholieke Universiteit Leuven in 2001. In 2001, he joined the ESAT-MICAS Laboratory at the Katholieke Universiteit Leuven as a research assistant of the Fund for Scientific Research-Flanders (Belgium) (F.W.O.-Vlaanderen). He is currently working towards a PhD. His main research interests are: pressure sensors, low power sensor interfaces, data acquisition systems and biotelemetry.

Bart Hermans was born in Vilvoorde, Belgium, in 1977. He received his BS degree in electro-mechanics from K.I.H. Denayer in 1999. In 2001, he received his MS degree in electrical engineering at the Katholieke Universiteit Leuven. Currently, he is a research assistant at the ESAT-MICAS Laboratories of the Katholieke Universiteit Leuven, where he is working towards a PhD degree. His main research interests are inductive powering, low power data transmission for biomedical applications and intelligent implantable monitoring systems.

Robert Puers was born in Antwerpen, Belgium, in 1953. He received his BS degree in electrical engineering in Ghent in 1974 and his MS degree at the Katholieke Universiteit Leuven in 1977, where he received his PhD degree in 1986. He is currently professor at the Katholieke Universiteit Leuven, Belgium, and Director of the Clean Room Facilities for Silicon and Hybrid Circuit Technology at the ESAT-MICAS Laboratories of the same University. He teaches courses of "microsystems and sensors", "biomedical instrumentation and stimulation", "technology for hospitals" and "electronics, automatization and IT". His main research interests are: biomedical implant systems (monitoring and stimulation), transducer and actuator principles, mechanical sensors (pressure, accelerometers, strain gauges, temperature, etc.), silicon micromachining; packaging and interconnection techniques (hybrids, hermetic and biocompatible sealing, etc.) and biotelemetry (inductive power delivery, bidirectional data communication). Prof. Puers is involved in the organization, reviewing and publishing activities of many conferences, journals and workshops in the field of biotelemetry, sensors, actuators, micromachining and microsystems. He is the author of more then 250 papers on biotelemetry, sensors or packaging in journals or international conferences.